SLIDING DISCHARGE STABILIZED BY THE WALL OF AN MHD CHANNEL

E. N. Vasil'ev, V. S. Slavin,
and P. P. Tkachenko

UDC 533.95

Detailed theoretical and experimental studies have been made [1] on the interaction between an arc discharge enclosed in an insulating channel with a gas flow in a magnetic field. Such a discharge acts as a form of plasma piston in the flow, since the gas can flow only near the walls, in the boundary-layer region. That type of interaction occurs in an MHD generator channel and in a railsotron. The plasma piston in an MHD generator is subject to an electrodynamic force $\mathbf{I}\times\mathbf{B}_0$, which retards the flow [2, 3], while in a railsotron, conversely one gets acceleration [4]. The discharge drift rate v_D relative to the gas flow coincides in direction with the $\mathbf{I}\times\mathbf{B}_0$ force, while in the case of an ideal impermeable piston, one should have $v_D = 0$. However, measurements [5, 6] show that under certain conditions, the discharge moves relative to the gas flow in a sense opposite to that of the electrodynamic force.

Here we consider how discharge drift arises and examine the structural dynamics under a retarding electrodynamic force.

We consider an arc discharge representing an impermeable piston in a supersonic gas flow. The current in the discharge region is maintained by the induced electric field, which is defined by $E = (K - 1)uB_0$, in which K is the load factor, which characterizes the external circuit, u the arc speed relative to the channel wall, and B_0 the external field induction. That type of arc occurs in magnetohydrodynamics as a self-maintaining current layer (T layer) [7].

We evaluate the various mechanisms producing the discharge region with the following MHD interaction parameters: pressure in flow $p \approx 0.1$ MPa, flow speed $u \approx 10^3$ m/sec, external induction $B_0 \approx 2$ T, arc size along axis $\delta \approx 0.1$ m, gas temperature in discharge region $T_D \approx 10^4$ K, electrical conductivity $\sigma \approx 10^3\ \Omega^{-1}\cdot m^{-1}$, and channel length $\ell \approx 1$ m. The arc residence time in the channel $\tau^* = \ell/u \sim 10^{-3}$ sec is comparable with the characteristic times in the dynamic processes: $\tau_F = \delta/\sqrt{\gamma RT_D} \sim 10^{-5}$—$10^{-4}$ sec, the force-balance settling time, $\tau_Q = c_p\rho T_D/(\sigma u^2 B_0^2) \sim 10^{-3}$ sec the gas heating time arising from Joule dissipation, and $\tau_\lambda = c_p\rho\delta^2/\lambda \sim 1$ sec the temperature-balance settling time due to thermal conduction. This relation shows that within the interval $\tau_F < t < \tau^*$, there is a nonstationary heat-balance settling process in the channel involving Joule dissipation and radiation. The convective energy losses to the walls at about 10^4 K are unimportant by comparison with the radiative losses [8], while there is no convective heat transfer from the discharge to the flow in the impermeable-piston model. The induced magnetic field is $B_{ind}/B_0 \approx (1 - K)R_m \approx 0.3\mu_0\sigma u\delta < 0.1$, so its effect can be neglected.

These estimates are used with the magnetogas-dynamic equations for the discharge region and $t > \tau_F$ to get the simplification

$$\rho dp/ds = \sigma(K-1)uB_0^2; \tag{1}$$

$$c_p\rho dT/dt - dp/dt = \sigma(1-K)^2u^2B_0^2 - q_R; \tag{2}$$

$$dx/ds = \rho^{-1}; \tag{3}$$

$$p = \rho RT; \tag{4}$$

$$q_R = \operatorname{div} H, \tag{5}$$

in which ρ is gas density, s the Lagrangian coordinate, and $H = \int_0^{\infty}\int_0^{\pi} J_\nu(\theta, \nu)\cos\theta d\theta d\nu$ the radiation flux density. The spectral radiation intensity J_ν is derived by solving the radiation

Krasnoyarsk. Translated from Zhurnal Prikladnoi Mekhaniki i Tekhnicheskoi Fiziki, No. 4, pp. 10-16, July-August, 1988. Original article submitted April 8, 1987.

0021-8944/88/2904-0467$12.50

transport equation for a planar radiating layer having an inhomogeneous temperature distribution along the axis:

$$\cos\theta dJ_\nu/ds = -\varkappa_\nu(J_\nu - B_\nu). \tag{6}$$

Here θ is the angle between the x axis and the radiation propagation direction, $\varkappa_\nu$ the mass spectral absorption coefficient, and B_ν the Planck function.

We supplement (1)-(5) with integral relations describing the flow of a nonconducting gas, which are necessary to determine the T-layer speed and specify the conditions at the boundaries of it. If there is force balance,

$$p_1(u) - p_2(u) = uB_0^2(1-K)\int_0^\delta \sigma(x)\,dx, \tag{7}$$

in which p_1 is the pressure behind the shock wave diverging from the T layer:

$$p_1 = p_0\left(\frac{2\gamma}{\gamma+1}M_1^2 - \frac{\gamma-1}{\gamma+1}\right); \tag{8}$$

with p_2 the pressure in the expansion wave:

$$p_2 = p_0(c_2/c_0)^{2\gamma/(\gamma-1)}. \tag{9}$$

The Mach number in the shock wave $M_1 = (u_0 - D)/c_0$ is calculated from the conservation of matter at it:

$$\frac{u_0 - D}{u - D} = \frac{\rho_1}{\rho_0} = \frac{(\gamma+1)M_1^2/2}{1+(\gamma-1)M_1^2/2}. \tag{10}$$

The speed of sound c_2 in the expansion wave is derived from the conservation of the Riemann invariant in a simple wave:

$$c_2 = c_0 - (\gamma-1)(u_0 - u)/2. \tag{11}$$

Then (7)-(11) can be used with the known $\sigma(x)$ to derive u uniquely.

The initial condition for (1)-(11) is a supersonic unperturbed flow having parameters p_0, T_0, and u_0, which are related to the retardation parameters and the Mach number in the unperturbed flow by $p_0 = p_s[1+(\gamma-1)M_0^2/2]^{-\gamma/(\gamma-1)}$, $T_0 = T_s[1+(\gamma-1)M_0^2/2]^{-1}$, $u_0 = M_0(\gamma RT_s)^{1/2}$. The initial parameters in the plasma region are specified by the scale δ_0 and temperature T_D.

The gas-dynamic and radiation-transport equations are solved together during iterations. The algorithm for solving a magnetogas-dynamic equation system has been described in [9]. The radiation fluxes have been determined by averaging the radiation-transport equations [10] on the basis that the transport equation is solved completely after a certain number of time steps. In our calculations, the numerical integration was based on 560 frequency ranges divided into 10 groups, together with 20 angular intervals. At the intermediate times, the magnetogas-dynamic equations were solved together with a multigroup averaged-equation derived from complexes integrated with respect to frequency and angle, which were computed from the complete solution to the transport equation. These averaged equations are exact in the sense that they give the same radiation pattern as the exact solution for a given temperature pattern.

The working-body thermodynamics may be described by an ideal-gas equation having effective adiabatic parameter $\gamma = 1.25$ and molecular weight 29. The conductivity $\sigma(T, p)$ and the absorption coefficient $k_\nu(T, p, \nu) = \rho\varkappa_\nu$ corresponded to those for an air plasma [11, 12].

Figures 1 and 2 show the current-layer formation for $M_0 = 2$, $p_S = 1$ MPa, $T_S = 3\cdot10^3$ K, and $K = 0.7$. The curves represent the following instants: 0) initial profile, 1) τ_F, 2) $1.5\cdot10^{-4}$, 3) $6\cdot10^{-4}$, 4) $1.2\cdot10^{-3}$, 5) $1.8\cdot10^{-3}$ sec. The initial isobaric temperature perturbation was specified as a sine wave. In time $t \sim \tau_F$, the current layer is retarded and a pressure difference arises across it; the bulk force produces an adiabatic structure in the plasma piston: in the high-pressure region, the gas is heated, whereas it is cooled in the expansion wave. In the subsequent evolution, the main part is played by the balance between Joule dissipation and radiative heat transfer. In time $t \sim \tau_Q$, the adiabatic structure is rearranged and a profile arises having peaks in the temperature and conductivity adjoining the expansion wave. Calculations with various initial conditions showed that the scale of the resulting T layer is almost independent of that in the initial perturbation, being completely determined by the flow parameters. It has been found [13] that a similar structure arises with a maximum current density in the expansion-wave region.

Figure 2 shows that for $t \gtrsim \tau_Q$, the conductivity peak is displaced into the expansion-wave region, while the conductivity falls in the high-pressure region. Consequently, the conducting zone begins to move (slide) relative to the gas flow at a speed of about 30 m/sec. This sliding relative to the nonconducting flow in a sense opposite to that of the electrodynamic force alters our view on the T layer as a formation localized in a certain mass of gas [14].

A sliding T layer can occur if there is heat transfer that raises the temperature in the nonconducting layers. However, such transfer of itself does not ensure that the conducting region slides. For example, no such effect was found in [15] in a discussion on T-layer formation by Joule dissipation and thermal conduction.

The sliding T layer can be explained as follows. The high-temperature central zone in T layer emits radiation, which is absorbed in the peripheral low-temperature parts. The less-dense gas in the expansion wave is heated much more rapidly than the dense gas adjoining the compression wave. When the gas is heated in the low-pressure region, the thermal ionization increases, and a current begins to flow, which completes the heating. In the high-pressure region, the hot gas has elevated emissivity, so the temperature there falls and the gas loses its conductivity. The two mechanisms together result in a dynamic equilibrium, and the current layer as a whole is displaced relative to the nonconducting flow in a sense opposite to that of $\mathbf{I}\times\mathbf{B}_0$. The sliding velocity is evidently overestimated in this model, because no allowance is made for any change in the specific heat of the gas with temperature.

A sliding discharge has also been observed in experiments with inert gas [6], where streamer displacement occurred in an MHD channel at a relative speed constituting 5% of the flow speed. A difference from a molecular gas was that the discharge drift here can be supported not by ordinary thermal heating but by radiative ionization transport.

It is difficult to perform a more detailed analysis on the T-layer structuring by radiative transport because the absorption coefficient has a highly nonlinear dependence on frequency, temperature, and pressure. At the same time, the $q_R = \mathrm{div}H$ distribution derived from the radiation-transport equation can be used for a model temperature profile with uniform pressure, which shows that bulk radiation occurs for the central regions in the plasma layer, whereas absorption predominates at the edges (Fig. 3). This q_R distribution enables one to simulate the radiation losses as the combined effects from the bulk emission in conjunction with thermal conduction represented by an effective thermal conductivity λ^*. The energy loss in that case is

$$q_R = 4\sigma_R\varepsilon(T, p, \delta)T^4/\delta - \lambda^*\partial^2T/\partial x^2, \qquad (12)$$

where σ_R is Stefan's constant, $\varepsilon(T, p, \delta)$ the emissivity of a hemispherical isothermal volume having radius δ, and $\lambda^* = \mathrm{const}$. The approach is similar to that in the modified diffusion approximation [16], in which the radiation is represented as a superposition of approximations for optically thick and optically thin bodies. Incorporating the energy loss as in (12) greatly simplifies the analysis, and the computations require much less time and memory.

Figures 4 and 5 show the T-layer structuring for $\lambda^* = 100\ \mathrm{W\cdot m^{-1}\cdot K^{-1}}$ for the same parameters, where the curves correspond to the following instants: 0) initial profile, 1) τ_F, 2) $5\cdot10^{-4}$, 3) 10^{-3}, 4) $3\cdot10^{-3}$, 5) $7\cdot10^{-3}$ sec. This loss model provides a drifting conducting zone, where the structuring is similar to that found from a calculation incorporating radiation transport. Quantitative correspondence can be provided by choosing $\lambda^*(T, p)$. That approach may be promising for two-dimensional treatments, in which it is difficult to use even radiation-transport equation averaging because of the vast amount of computational time required.

A comparison has been made with the bulk emission model (with $\lambda^* = 0$), which indicates that bulk radiative losses have the largest effect in the central hot current-layer zone. The blackness ε is almost directly proportional to the pressure for the characteristic parameters, so the interaction produces a temperature peak in the low-pressure region. The stabilized structure produced by bulk radiative losses is [9, 17] independent of the initial perturbation shape and scale, being completely determined by the process parameters.

The effective thermal conductivity mechanisms has an effect mainly near the boundaries of the T layer, where the temperature gradients are largest, while it has virtually no effect on the energy balance for the central zone. Therefore, conducting-zone drift is provided by that mechanism, which heats the nonconducting gas. This is confirmed by the relation between the discharge drift rate and λ^* (Fig. 6): at first, as λ^* increases, v_D increases

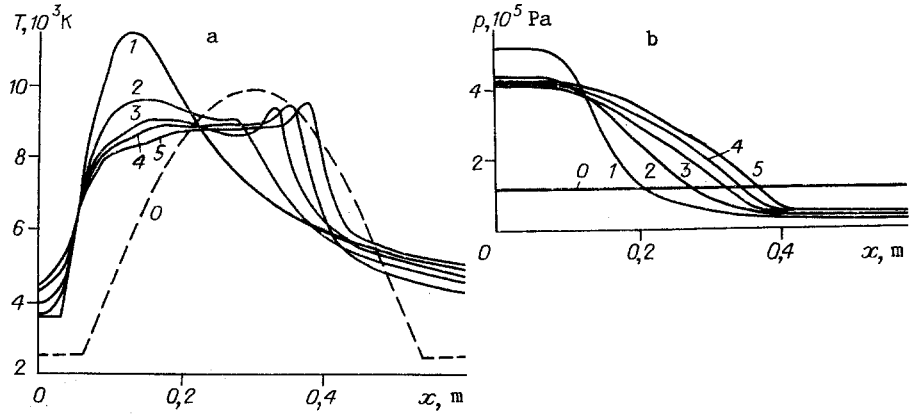

Fig. 1

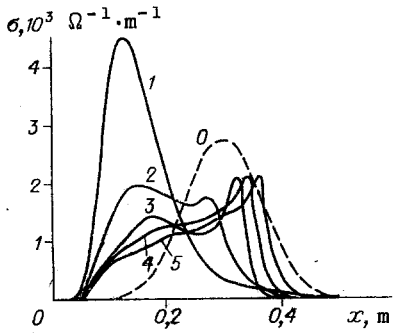

Fig. 2

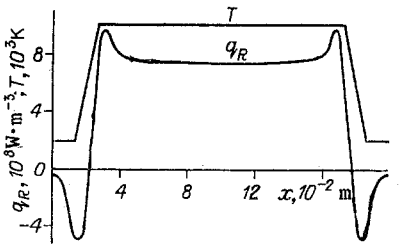

Fig. 3

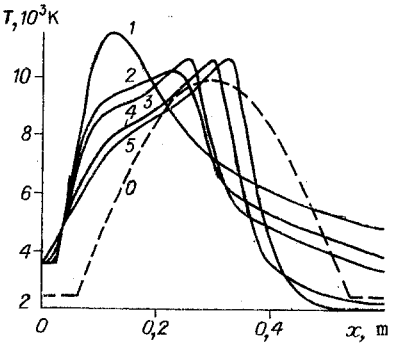

Fig. 4

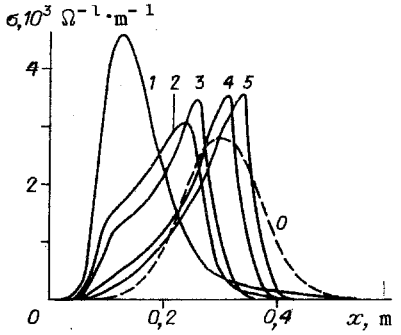

Fig. 5

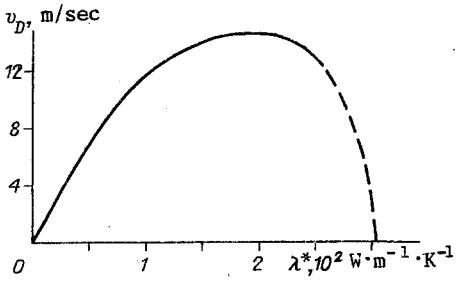

Fig. 6

because cold gas is heated more, but as λ^* increases further, the T-layer boundaries become very diffuse and the temperature gradients decrease, which first stabilizes the speed and then reduces it. The dashed line shows λ^* such that the energy losses due to effective conduction increase so much that the T layer breaks up because the gas cools and loses its conductivity. For a real value for the conductivity $\lambda \approx 1$ W·m^{-1}·K^{-1}, the conduction mechanism has virtually no effect on the T-layer structuring.

Radiation transport can thus be incorporated into a model for an impermeable plasma piston interacting with a magnetic field to demonstrate the current-layer drift relative to the gas flow in a sense opposite to that of the electrodynamic force, which enables one to establish the mechanisms supporting the drift. Of course, a real plasma piston is permeable to the nonconducting gas, at least in the boundary-layer region, so in measurements, the discharge begins to move in the opposite sense to $\mathbf{I}\times\mathbf{B}_0$ if the drift speed exceeds the flow speed. Clearly, that is possible above a current I at which the discharge column covers the cross section and provides a sufficiently powerful radiation flux.

LITERATURE CITED

1. G. R. Jones and M. T. C. Fang, "The physics of high-power arcs," Rep. Progr. Phys., 43, No. 12 (1980).

2. V. A. Derevyanko, V. S. Slavin, and V. S. Sokolov, "An MHD generator containing a T layer," Proceedings of the 8th Intern. Conference on MHD Energy Conversion [in Russian], Vol. 2, Moscow (1983).
3. J. M. Wetzer, "Microscopic and macroscopic streamer parameters of a noble gas linear MHD generator," 22nd Symposium on Engineering Aspects of MHD, Starkville, USA (1984).
4. S. V. Kukhtetskii, A. D. Lebedev, and V. A. Lyubochko, "Motion of a high-current discharge in a dense gas," Teplofiz. Vysok. Temp., 23, No. 3 (1985).
5. A. D. Lebedev, V. I. Nazaruk, et al., "A high-current arc discharge in a magnetic field," in: Low-Temperature Plasma Generators [in Russian], Part 1, Kaunas (1986).
6. J. C. N. Bosma, A. Veefkind, J. F. Uhlenbuch, and L. H. Rietjens, "Experimental investigation on the gasdynamic interaction between streamers and background gas in a noble gas MHD generator," 23rd Symp. on Engineering Aspects of MHD, Pennsylvania (1985).
7. A. N. Tikhonov, A. A. Samarskii, et al., "The nonlinear effect in the formation of a self-maintaining hot conducting gas layer in nonstationary magnetohydrodynamics," Dokl. Akad. Nauk SSSR, 173, No. 4 (1967).
8. V. A. Derevyanko, V. S. Slavin, and V. S. Sokolov, "A magnetohydrodynamic electricity generator based on brown-coal gasification products," Zh. Prikl. Mekh. Tekh. Fiz., No. 5 (1980).
9. E. N. Vasil'ev, V. A. Derevyanko, and V. S. Slavin, "A stabilized current layer," Teplofiz. Vysok. Temp., 24, No. 5 (1986).
10. I. V. Nemchinov, "The averaged radiation-transport equations and applications in gasdynamic treatments," Prikl. Mat. Mekh., 34, No. 4 (1970).
11. I. A. Sokolova, "Transport coefficients and collision integrals for air and air components," in: Physical Kinetics [in Russian], ITPM SO AN SSSR, Novosibirsk (1974).
12. I. V. Avilova, L. M. Biberman, et al., The Optical Parameters of Hot Air [in Russian], Nauka, Moscow (1970).
13. V. A. Derevyanko, V. S. Sokolov, et al., "Experimental investigation of self-maintained current layer in MHD channel," 9th Intern. Conf. on MHD Electrical Power Generation, Tsukuba, Japan (1986), Vol. 4.
14. N. P. Gridnev, S. S. Katsnel'son, and V. P. Fomichev, Inhomogeneous MHD Flows Containing T Layers [in Russian], Nauka, Novosibirsk (1984).
15. N. V. Sosnin and A. P. Favorskii, Steady-State Magnetohydrodynamic T-Layer Structures [in Russian], No. 64, Preprint, Inst. Prikl. Mat. Akad. Nauk SSSR, Moscow (1976).
16. S. Trogott, "The radiative heat flux potential for a nongray gas," RTK, 4, No. 3 (1966).
17. E. N. Vasil'ev, V. V. Ovchinnikov, and V. S. Slavin, "The phase diagram for a stabilized current layer in an MHD generator channel," Dokl. Akad. Nauk SSSR, 290, No. 6 (1986).

SIMULATING THE CATHODE REGION IN A STATIONARY SELF-MAINTAINED GLOW DISCHARGE

V. A. Shveigert and I. V. Shveigert

UDC 537.52

The cathode region is the most important part of a gas discharge as it is responsible for the very existence of it [1]. The electric fields are strong and highly inhomogeneous there, and consequently there is a nonlocal relation between the electron distribution and the field strength [2], which substantially complicates examining that region. At present, there is no self-consistent analysis for that region that incorportes the nonlocal electron distribution and the relations between the various parts of the cathode region: the cathode layer, the negative glow, and the Faraday dark space. In [3, 4], the layer was examined most fully, but the discussion concerned short discharge gaps, where there is virtually no weak-field region. Here we present a model that treats the cathode region in a self-consistent fashion. The results are briefly compared with ones for discharges in helium.

We consider the case of low cathode potential differences ($U_c \leqslant 500$ V) and medium gas-atom concentrations ($N \sim 10^{16}$-10^{17} cm^{-3}), for which one can neglect the participation of fast ions and neutral particles (in direct ionization, as well as kinetic electron ejection from

Novosibirsk. Translated from Zhurnal Prikladnoi Mekhaniki i Tekhnicheskoi Fiziki, No. 4, pp. 16-23, July-August, 1988. Original article submitted March 12, 1987.

0021-8944/88/2904-0471$12.50